Structure-Based Drug Design of a Novel Family of PPARγ Partial Agonists: Virtual Screening, X-ray Crystallography, and in Vitro/in Vivo Biological Activities

I-Lin Lu,[†,‡,⊥] Chien-Fu Huang,[†,⊥] Yi-Hui Peng,[†] Ying-Ting Lin,[†] Hsing-Pang Hsieh,[†] Chiung-Tong Chen,[†] Tzu-Wen Lien,[†] Hwei-Jen Lee,[§] Neeraj Mahindroo,[†] Ekambaranellore Prakash,[†] Andrew Yueh,[†] Hsin-Yi Chen,[†] Chandra M. V. Goparaju,[†] Xin Chen,[†] Chun-Chen Liao,[∥] Yu-Sheng Chao,[†] John T.-A. Hsu,[†,*] and Su-Ying Wu[†,*]

Division of Biotechnology and Pharmaceutical Research, National Health Research Institutes, Taipei, Taiwan, ROC, Graduate Institute of Life Sciences, National Defense Medical Center, Taipei, Taiwan, ROC, Department of Biochemistry, National Defense Medical Center, Taipei, Taiwan, ROC, and Department of Chemistry, National Tsing Hua University, Hsinchu 300, Taiwan, ROC

Received November 10, 2005

Peroxisome proliferator-activated receptor γ (PPARγ) is well-known as the receptor of thiazolidinedione antidiabetic drugs. In this paper, we present a successful example of employing structure-based virtual screening, a method that combines shape-based database search with a docking study and analogue search, to discover a novel family of PPARγ agonists based upon pyrazol-5-ylbenzenesulfonamide. Two analogues in the family show high affinity for, and specificity to, PPARγ and act as partial agonists. They also demonstrate glucose-lowering efficacy in vivo. A structural biology study reveals that they both adopt a distinct binding mode and have no H-bonding interactions with PPARγ. The absence of H-bonding interaction with the protein provides an explanation why both function as partial agonists since most full agonists form conserved H-bonds with the activation function helix (AF-2 helix) which, in turn, enhances the recruitment of coactivators. Moreover, the structural biology and computer docking studies reveal the specificity of the compounds for PPARγ could be due to the restricted access to the binding pocket of other PPAR subtypes, i.e., PPARα and PPARδ, and steric hindrance upon the ligand binding.

Introduction

Peroxisome proliferator-activated receptors (PPARs[a]) are ligand-activated transcription factors belonging to the nuclear hormone receptor (NHR) superfamily.[1,2] Three PPAR subtypes, encoded by distinct genes, are designated as PPARα, PPARδ, and PPARγ. Several recent reviews have described the biological functions of these NHRs in controlling glucose and lipid metabolism.[3−5] PPARα is expressed mainly in the liver, and its biological role is closely related to fatty acid metabolism and peroxisome proliferation.[6] PPARδ is expressed in most cell types; several studies indicate that PPARδ agonists play important roles in dyslipidemia,[7] cancer treatment,[8] and differentiation of cells within the central nervous system.[9] Interestingly, a recent report shows that PPARδ agonists could stimulate muscle fiber transformation and enhance physical endurance.[10] PPARγ is abundant in adipose tissue and plays an important role in adipocyte differentiation. Studies also show that PPARγ is the receptor for a well-known class of antidiabetic drugs, thiazolidinedione (TZD).[11]

The advent of the TZD antidiabetic drugs, e.g. rosiglitazone (Figure 1) and pioglitazone, has led to extensive research in the area of antidiabetic drug discovery and development. However, despite their effectiveness in treating diabetes, TZD drugs possess undesirable side effects, such as increased adiposity, edema, significant cardiac hypertrophy, and the risk of heart failure. Thus, there is an urgent need to discover PPARγ agonists with improved therapeutic profiles.

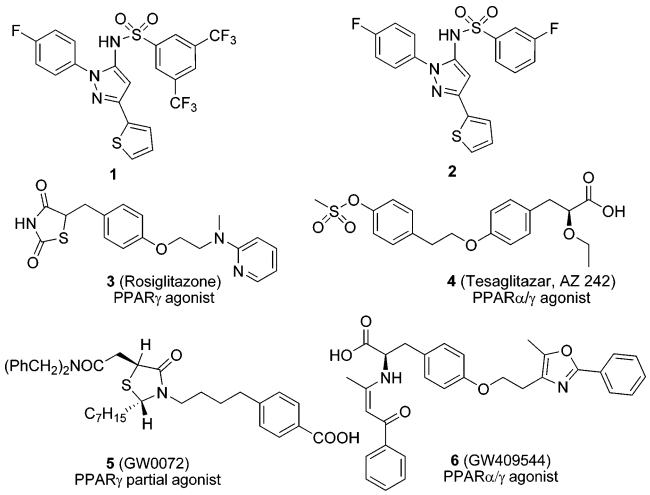

Figure 1. PPAR agonists.

Several alternative approaches have been taken to seek for new classes of PPAR ligands, including PPARα/γ dual agonists, PPAR$\alpha/\gamma/\delta$ pan agonists, and PPARγ partial agonists. Various PPAR dual agonists and pan agonists have been developed by several pharmaceutical companies and some of them such as muraglitazar[12] and tesaglitazar[13] (Figure 1) are in advanced stages of clinical development. However, the development of several PPAR dual agonists has been terminated in clinical trials as a long-term safety study showed these compounds induce malignant tumors in mice.[14,15] Therefore, the safety issue and therapeutic benefit of dual and pan agonists still require further investigation before FDA approves any dual or pan PPAR agonist.

* To whom correspondence should be addressed: Su-Ying Wu, Tel.: 886−37−246166 ext 35713; E-mail: suying@nhri.org.tw; Fax: 886-37-586456. John T. A. Hsu, Tel.: 886-37-246166 ext 35717; E-mail: tsuanhsu@nhri.org.tw; Fax: 886-37-586456.

† National Health Research Institutes.

‡ Graduate Institute of Life Sciences, National Defense Medical Center.

§ Department of Biochemistry, National Defense Medical Center.

∥ Department of Chemistry, National Tsing Hua University.

⊥ The authors contributed equally to this work.

[a] Abbreviations used: PPARγ, peroxisome proliferator-activated receptor γ; AF-2 helix, activation function helix; NHR, nuclear hormone receptor; TZD, thiazolidinedione; PPARγ -LBD, PPARγ ligand binding domain; GST, glutathione S-transferase; SPA, Scintillation proximity assay; DMEM, Dulbecco's modified Eagle's medium; FCS, fetal calf serum.

10.1021/jm051129s CCC: $33.50
Published on Web 04/07/2006

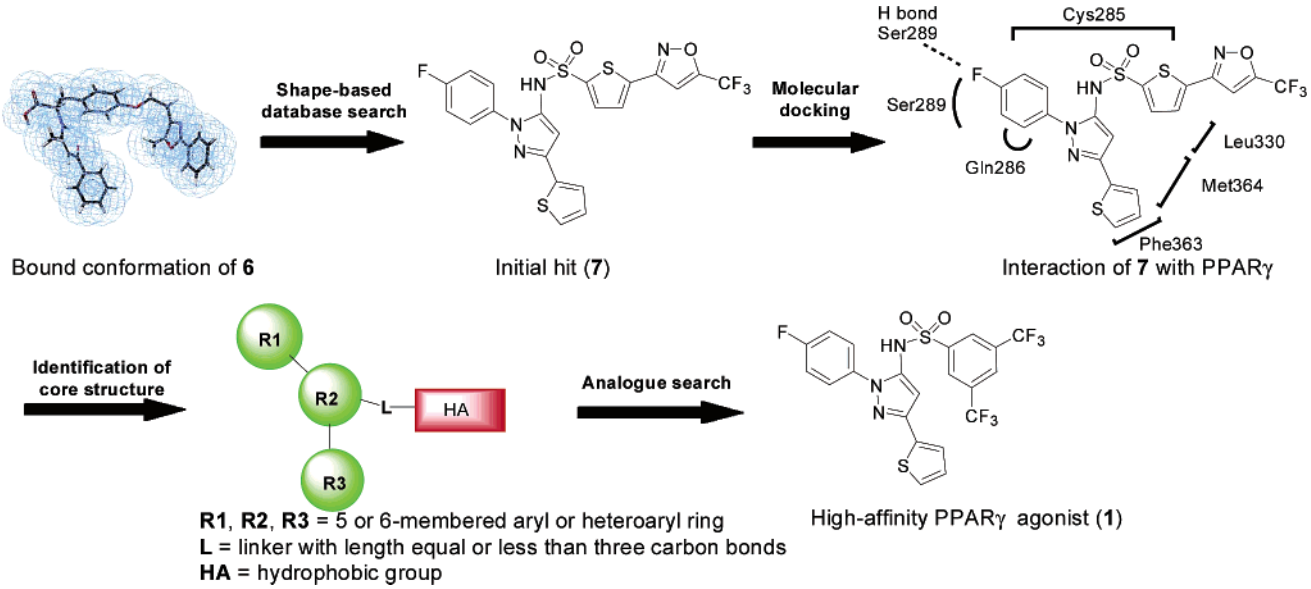

Figure 2. Discovery of high-affinity PPARγ agonists by structure-based virtual screening. The conformation of **6** bound in the active site of PPARγ was used as the pharmacophore to perform shape-based database search. Compound **7** with minimized conformations similar to **6** and IC_{50} of 175 nM was identified as the hit compound. A molecular docking study reveals the aromatic rings of compound **7** made hydrophobic interactions with the surrounding residues, Cys285, Gln286, Ser289, Leu330, Phe363, and Met364. A H-bonding interaction was formed between the fluorine atom and Ser289, indicated by the dotted line. The knowledge obtained from the molecular docking study was applied as the criteria to define the core structure. By analogues search, compound **1** with an IC_{50} of 22.7 nM, a 7-fold increased potency over its parent compound, was identified as a potent PPARγ agonist.

A recent study shows PPARγ partial agonists exhibit fewer side effects as compared to full agonists. One non-TZD PPARγ agonist, nTZDpa (5-chloro-1-(4-chlorobenzyl)-3-phenylsulfanyl-1*H*-indole-2-carboxylic acid), has been reported recently to overcome the problems of weight gain and avoid cardiac hypertrophy in C57BL/6 mice.[16] The same report also indicated that partial agonists might be the key to decrease the side effects seen with TZD compounds. Another partial agonist, LSN862 ((*S*)-2-methoxy-3-{4-[5-(4-phenoxy)pent-1-ynyl]phenyl}-propionic acid), demonstrated better antidiabetic activity and fewer side effects in animal studies.[17] Although PPAR partial agonists have potential to gain therapeutic advantage over existing drugs in the treatment of type 2 diabetes, it is not yet well-defined how partial agonists interact with the PPARγ and what genes they turn on or off. Some researchers have proposed that partial agonists bind to PPARγ in a different manner which leads the protein to recruit different kind of cofactors and consequently to regulate diverse sets of genes. All of these studies give partial agonists a distinct clinical profile as compared to full agonists and suggest the exploration of PPARγ partial agonists is a promising approach to develop antidiabetic drugs with more desirable therapeutic properties.

Structural biology has emerged as a powerful technology to study how a compound activates a protein, since if the protein−ligand interaction can be "visualized" at atomic resolution, the key residues involved in binding the ligand would be revealed. Several structures of PPARγ ligand binding domain (PPARγ-LBD) in complex with various ligands have been solved recently.[18−21] The structure of the PPARγ-LBD consists of a helical sandwich and four small β-strands. The ligand-binding site is located in the bottom half of the overall structure and is Y-shaped with a volume of about 1300 Å. As revealed in protein−ligand complex structures, PPARγ full agonists, such as rosiglitazone and tesaglitazar,[22] interact with the AF-2 helix through a thiazolidinedione ring or a carboxylic acid moiety, leading to the recruitment of coactivators.[18,19] In comparison, **5** (Figure 1), a PPARγ partial agonist, binds to PPARγ at a position far away from the conserved hydrogen bonding site and has no interaction with the AF-2 helix.[23]

In this study, pyrazol-5-ylbenzenesulfonamides were identified through the structure-based virtual screening as a novel class of PPARγ ligands. Biological data from binding and transactivation assays characterized compound **1** (*N*-[1-(4-fluorophenyl)-3-(2-thienyl)-1*H*-pyrazol-5-yl]-3,5-bis(trifluoromethyl)benzenesulfonamide) and compound **2** (3-fluoro-*N*-[1-(4-fluorophenyl)-3-(2-thienyl)-1*H*-pyrazol-5-yl]benzenesulfonamide) (Figure 1) as high affinity and selective agonists of human PPARγ. They were further subjected to extensive characterization, including crystal structure determinations, functional assays, and in vivo studies. The two compounds functioned as partial agonists, and the key determinants for their selectivity among the three PPAR subtypes are also discussed in this paper.

Results and Discussion

Identification of a Novel Family of PPARγ Ligands by Structure-Based Virtual Screening. In the first round of virtual screening, a shape-based database search was performed using the program Catalyst 4.7. The method relies on the principle that a molecule has to adopt a specific 3D-conformation upon binding to its receptor. A smaller set of compounds with similar conformation but diverse topology to the reference ligand was then selected from a large database.

The conformation of **6** (Figure 1) bound in the active site of PPARγ (PDB code: 1K74) was used as the pharmacophore. [19] The bound conformation of **6**, which adopted a ∩-shape (an inverted U shape) to bind to the protein, was used to screen the Maybridge database, a database of commercially available small molecules. Out of ca. 62000 compounds, 163 with minimized conformations similar to the ∩-shape were selected and screened by the scintillation proximity assay (SPA) for PPARγ binding. One of the selected compounds, **7** (*N*-[1-(4-fluorophenyl)-3-(2-thienyl)-1*H*-pyrazol-5-yl]-5-[5-(tri-fluoromethyl)isoxazol-3-yl]-thiophene-2-sulfonamide (Figure 2), showed significant binding

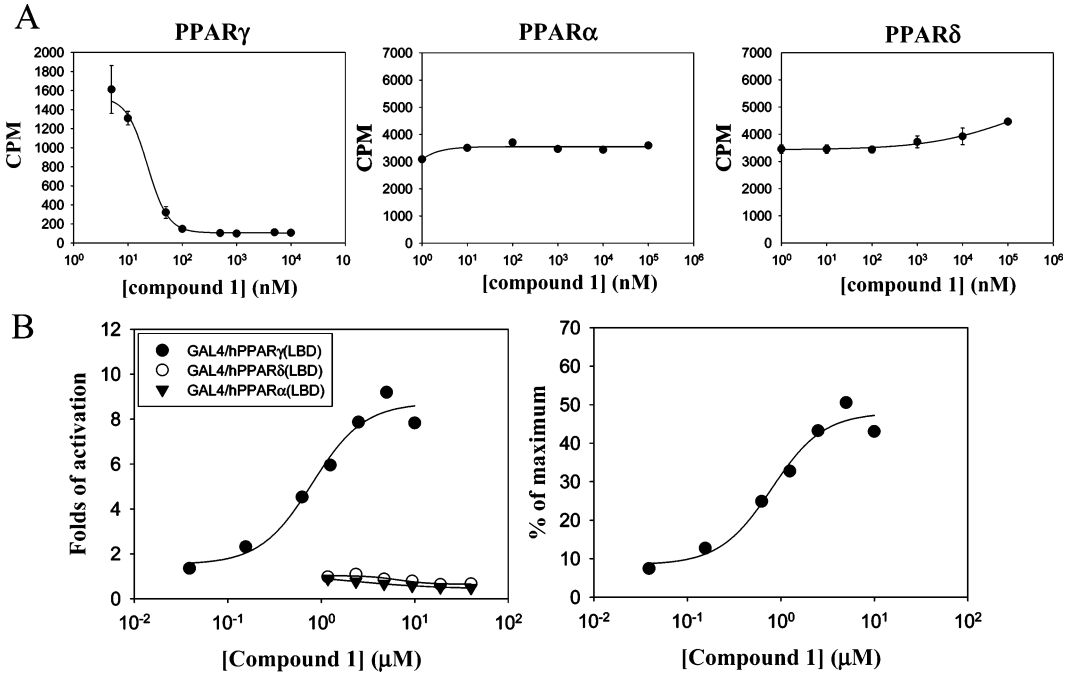

Figure 3. The binding affinity and transcriptional activation of compound **1**. (a) The binding affinity of compound **1** to PPARγ was determined by SPA assay. Compound **1** at various concentrations was added into the SPA binding buffer containing PPARγ and a radio-labeled ligand, [^{3}H]-rosiglitazone. Compound **1** replaced [^{3}H]rosiglitazone upon its binding to PPARγ, leading to the decreased scintillant activation as revealed by counts per minute (CPM). IC_{50} of Compound **1**, obtained from a linear least-squares fit from the plot, was 22.7 nM. In contrast, CPM numbers remained unchanged with the addition of increased concentration of compound **1** to PPARα and PPARδ, suggesting that compound **1** was not able to bind to both proteins. (b) The transcriptional activity of compound **1** on PPARα (triangle), PPARδ (open circle), and PPARγ (circles) were determined in Huh-7 cells. The luciferase activities in the cell extracts were measured after incubation with increasing concentrations of compound **1**. Compound **1** showed a dose-dependent transcriptional activity on PPARγ whereas it has no transcriptional activity on PPARα and PPARδ. Results are expressed as percent of maximum, where maximum transcriptional activity was determined by treatment with 2 μM rosiglitazone in PPARγ transactivation assay.

affinity with an IC_{50} of 175 nM and was subjected to a second round of virtual screening. In the second round, compound **7** was first docked into the active site of the protein using the PPARγ/**6** complex structure as a template. The predicted model showed the thiophene group of compound **7**, next to the pyrazole group, extended deep into the hydrophobic pocket formed by helices 3 and 7 and made a $\pi-\pi$ stacking interaction with Phe363. The pyrazole group and sulfonamide moiety made close contacts with Met364 and Leu330 while the other thiophene group, connected to the sulfonamide moiety, and the fluorophenyl group formed strong hydrophobic interactions with Cys285. In addition, the fluorine atom substituted in the phenyl group formed one H-bond with Ser289. Finally, the 5-trifluoromethylisoxazole group fitted into the entrance of the binding pocket but had no interaction with the protein. As revealed in the docking model, all the aromatic rings of compound **7**, with the exception of the isoxazole group, made major interactions with the protein. Therefore, the four aromatic rings, with the isoxazole ring excluded, together with the sulfonamide moiety were identified as the scaffold for a further analogue search. Several criteria were applied in the analogue search (Figure 2). Three aromatic rings, the thiophene, pyrazole, and phenyl, could be individually replaced by a 5- or 6-membered aryl or heteroaryl ring. The sulfonamide group, that functions as a linker, could be substituted with other linkers with a length equal to or less than three C−C bonds, e.g. C(O)N(H), CH_2CH_2. Moreover, the thiophene group which is adjacent to the sulfonamide group and forms strong hydrophobic interactions with Cys285, could be replaced by hydrophobic groups, such as alkyl, alkenyl, alkynyl, aryl, and heteroaryl. Thirty-seven compounds that fulfilled the above criteria were selected from the Maybridge database, and their binding affinities were evaluated by SPA assay. Out of 37 compounds, compound **1** showed the strongest binding affinity with an IC_{50} of 22.7 nM, displaying a 7-fold increased potency over its parent compound **7**. Moreover, compound **1** is smaller and has a lower molecular mass, which made it as an attractive lead for further optimization in search for a drug candidate. Therefore, compound **1** was subjected to further characterization by various functional assays and structural studies. In addition, compound **2** with a highly similar structure to compound **1** was also included in this study.

Biological Activity. Compound **1** is a high affinity PPARγ ligand as revealed by SPA assay. In the SPA assay, when a test compound binds to the protein binding pocket it displaces the bound radio-ligand, [^{3}H]rosiglitazone, lowering the bound radioactivity. Compound **1** displaced PPARγ -bound [^{3}H]-rosiglitazone with an IC_{50} value of 22.7 nM. In contrast, compound **1**, in concentrations up to 10 μM, did not show any apparent binding affinity toward PPARα and PPARδ in charcoal and SPA binding assays, respectively (Figure 3A). These results showed that compound **1** is a potent and specific PPARγ ligand. In similar experiments, the analogous compound **2** bound to PPARγ with an IC_{50} of 512 nM and showed no binding affinity toward PPARα or PPARδ, suggesting compound **2** is also a selective PPARγ ligand but less potent than compound **1**.

The GAL4-PPARγ transactivation assay was employed to evaluate the biological function of compounds **1** and **2**. Huh-7 cells were transfected with mixes of GAL4/PPARγ-LBD expression plasmid, $(UAS)_5$-TK-luc reporter plasmid, and pSV40−Ren plasmid as internal control. When transfected cells were treated with compound **1**, dose-dependent PPARγ transcriptional activity was evident as indicated by the reporter luciferase gene (Figure 3B). Compound **1** was specific for the transcriptional activation of GAL4/PPARγ-LBD, since it did

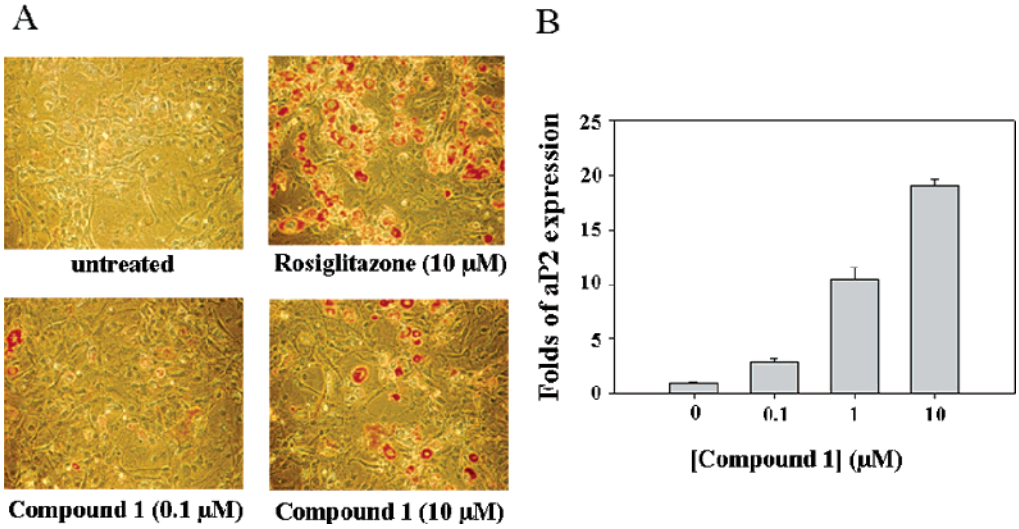

Figure 4. Compound **1** induced 3T3-L1 preadipocyte differentiation and increased aP2 mRNA expression. (a) Confluent 3T3-L1 preadipocytes were treated with 10 μM of rosiglitazone, 0.1 μM of compound **1**, and 10 μM of compound **1**, respectively. Following the treatment of compounds, 3T3-L1 cells were stained by Oil-red O. Increased concentration of compound **1** result in more adipocyte differentiation. Rosiglitazone treatment showed most potent adipogenic effect, as indicated by the intensive Oil-red staining. (b) Compound **1** could increase the expression level of aP2 mRNA. When 3T3-L1 cells were treated with compound **1**, mRNA expression levels in cells increased in a dose-dependent manner and an approximately 20-fold increase in aP2 mRNA levels were achieved when cells were treated with 10 μM of compound **1**. The results shown here are means from duplicate determinations from two independent experiments.

not induce any transcriptional activity mediated by either GAL4/PPARα-LBD or GAL4/PPARδ-LBD. The EC_{50} of compound **1** for transcriptional activation of GAL4/PPARγ-LBD cells was 0.78 ± 0.09 μM. Interestingly, the maximum transcriptional activity achieved by compound **1** was only 50% of the maximal effect achieved by the PPARγ full agonist, rosiglitazone at 2 μM, indicating that compound **1** is a partial agonist. In a similar experiment, compound **2** induced transcriptional activity of PPARγ with an EC_{50} of 1.75 ± 0.19 μM but to a lesser extent, the maximum transactivaiton being only to 31% of levels produced by rosiglitazone at 2 μM. Like compound **1**, compound **2** also did not show any activity in the GAL4/PPARα-LBD or GAL4/PPARδ-LBD transactivation assay.

Compound **1** was further characterized for its ability to promote adipocyte differentiation. Preadipocyte cells can be converted to mature adipocytes by PPARγ agonists, as monitored by the increase in Oil-red O staining and the expression of adipose fatty acid-binding protein 2 (aP2). As shown in Figure 4A, rosiglitazone stimulated adipocyte differentiation as indicated by intensive Oil-red O staining of cytoplasmic fat droplets in the 3T3-L1 cells. In the control experiment, hardly any red cells were visible in the untreated cells. When the cells were incubated with 0.1 μM of compound **1**, a few cells became red after Oil-red O staining. On increasing the concentration of compound **1** to 10 μM, a greater number of red-stained cells were observed but the amount was less than that seen in cells treated with rosiglitazone at 10 μM (Figure 4A). To examine further the ability of compound **1** to enhance adipocyte differentiation, the expression levels of aP2 mRNA were analyzed after treatment with various concentrations of compound **1**. As shown in Figure 4B, the expression level of aP2 mRNA was increased in a dose-dependent manner and an approximately 20-fold increase in aP2 mRNA levels was achieved upon treatment with 10 μM. By comparison, rosiglitazone at 10 μM increased the expression level of aP2 mRNA 35-fold. As revealed in both the Oil-red O staining and the aP2 expression experiments, compound **1** was able to stimulate adipocyte differentiation but showed weaker adipogenic activity than rosiglitazone, a classic PPARγ full agonist. These results for compound **1** may reflect its relative transcriptional activity for PPARγ and its function as a partial PPARγ agonist.

Table 1. X-ray Data Collection and Structure Refinement

	compound **1**	compound **2**
resolution (Å)	20−2.3	30−2.54
unit cell$P2_1(\alpha = \gamma = 90°)$	$a = 56.301$	$a = 56.419$
	$b = 88.897$	$b = 88.805$
	$c = 58.451$	$c = 58.258$
	$\beta = 90.80°$	$\beta = 89.99°$
total reflections observed	377652	154716
unique reflections	25799	18872
multiplicity	14.63	8.198
R_{merge}% (outer shell)	4.7(26.2)	8.1(36.4)
$\langle I/\sigma(I)\rangle$ (outer shell)	20.34(3.81)	13.81(3.72)
completeness % (outer shell)	99.8 (100.0)	99.1(99.9)
R_{work}%	23.8	21.63
R_{free}%	29.3	26.41
RMS bonds (Å)	0.008	0.008
RMS angles (deg)	1.796	1.978

X-ray Structures of PPARγ−Ligand Complexes. The refinement statistics of the two PPARγ-LBD−ligand complex structures, PPARγ/ compound **1** and PPARγ/compound **2** are shown in Table 1. The electron density maps of PPARγ LBD are clear, except for some disordered regions that include residues 264−273 in both monomers and residues 468−477 in monomer B. The loop of residues 264−273 is located at the entrance of the ligand-binding site and is highly flexible in all published structures. Its flexibility could probably allow the access of a ligand to the binding pocket of PPARγ. The protein structure is very similar to that of the apo-protein with the exception of Phe282, Leu330, Phe363, and Met364 in the binding site that adopt different conformations to allow a better fit with the ligand.

The electron density maps of compound **1** and compound **2** bound in the binding site are very clear, and the model of the compounds fit well into the density maps. The complex structures reveal these two ligands bind to PPARγ in a large hydrophobic pocket close to the AF-2 helix and formed by helices 3, 7, and 10 (Figure 5). This pocket is sometimes referred as the "benzophenone" pocket as seen in the PPARγ/farglitazar complex structure.[24]

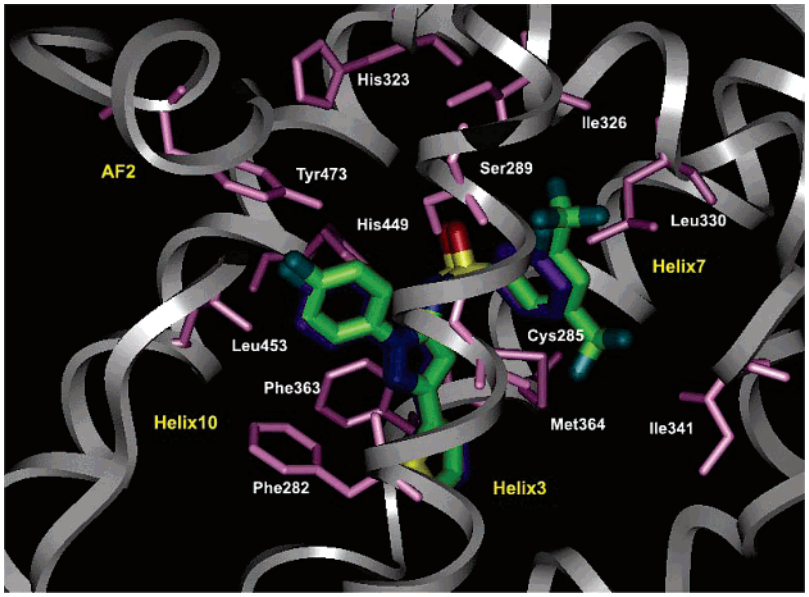

Figure 5. The structures of PPARγ ligand binding domain in complex with compound **1** (green) and compound **2** (purple). Compound **1** and compound **2** bind to PPARγ in a large hydrophobic pocket formed by helices 3, 7, and 10. All aromatic rings of compound **1** and compound **2**, except the phenyl ring connected to the sulfonamide in compound **2**, have extensive $\pi-\pi$ stacking and hydrophobic interactions with the surrounding protein residues, particularly with Phe363. Key interacting residues are labeled.

The chemical structure of compound **1** can be subdivided into five groups for discussion of its interactions with the protein (Figure 5). The first group is the thiophene group that inserts deep into the hydrophobic pocket making hydrophobic contacts with Phe282, Phe360, and Phe363. The second group is the pyrazole group, which forms strong $\pi-\pi$ interaction with Phe363. The hydrophobic interactions with Phe363 are seen in the tyrosine-based ligand but not in the TZD compounds and contribute the major interactions with the protein. The third moiety, a *p*-fluorophenyl group, binds to PPARγ at the top of the hydrophobic pocket and next to the AF-2 helix. The region consists of Phe282, Leu453, Leu465, Leu469, and Gln286, all of which interact strongly with the phenyl moiety. Notably, the phenyl group is the closest moiety to the AF-2 helix, but it makes neither strong hydrophobic nor H-bonding interactions with this functional helix. Only the fluorine atom attached to the phenyl ring has a weak van der Waals interaction with Tyr473. In contrast, all published full agonists, including TZD and the tyrosine-based ligands, have strong H-bonding interactions with Tyr473 in the AF-2 helix. The absence of interactions with the AF-2 could provide the structural basis for the partial agonist functionality of compound **1**. The fourth group is the sulfonamide group that serves as a linker between two of the aromatic groups in compound **1**. Interestingly, the sulfonamide group does not make any interactions with PPARγ, suggesting that the linker could be replaced by other groups of similar length without losing any of the binding affinity. The fifth group is the phenyl ring with two meta-substituted CF_3 groups. This phenyl ring forms strong hydrophobic interactions with PPARγ, particularly with Leu330 and Met364, and also make close contacts with Arg288, Ile326, Val 339, and Ile341.

As can be seen from the above discussion, all interactions of compound **1** with PPARγ are hydrophobic and there is no H-bonding interaction involved in the ligand binding. The sulfonamide group, does provide H-bonding interactions in compound **1**, is unable to make H-bonding interactions although it is only 4 Å away from the conserved H bond network formed by His449, His323, Tyr473, and Ser289. The lack of H-bonding interactions is a unique feature for compound **1** since all previously reported PPARγ ligands form at least one H-bond with the protein.

Comparison of Compounds 1 and 2 Complex Structures. Compound **2** is an analogue of compound **1** and its complex structure with PPARγ has been solved by the same procedure as for compound **1**. The chemical structure of compound **2** is very similar to that of compound **1**. The difference between them is in the substitution of the phenyl ring (Figure 1). However, despite their high similarity, they do exhibit different biological activity. As shown in the PPARγ SPA assay, the binding affinity of compound **1** is 10-fold stronger than that of compound **2**. Superimposition of the ligand complex structures reveals the structural basis for the difference in binding affinity (Figure 5). The position of compound **2** superimposes well with that of compound **1** except for the movement of the phenyl ring. In compound **2**, there is no interaction between the phenyl ring with the surrounding protein residues. However, in compound **1**, the phenyl ring slightly shifts to improve the fit with the protein. The phenyl ring and two CF_3 groups of compound **1** form strong interactions with Arg288, Ile326, Leu330, Val339, and Met364. The additional interactions of compound **1** with the protein, particularly those with Leu330 and Met364, account for its increased binding affinity compared to compound **2**. Moreover, on the basis of our comparison of the compounds **1** and **2** complex structures, we suggest other ring substitutions with hydrophobic groups, such as methyl or ethyl, may increase the binding affinity since most of the protein residues near the phenyl ring are hydrophobic in character, namely Ile326, Leu330, Val339, and Ile341.

Comparison of PPARγ Full Agonists Binding Modes. There are now around 10 published X-ray structures of small-molecule agonists complexed with PPARγ. Compared to all of these available complex structures, compounds **1** and **2** bind to PPARγ in a distinct manner (Figure 6). Rosiglitazone and tesaglitazar are PPARγ full agonists and represent a typical topology for PPARγ ligands, i.e., head, linker, and tail. In comparison, compounds **1** and **2** have different chemical scaffolds and interact differently with the protein. First, the head of the PPARγ full agonists, typically a thiazolidinedione or a

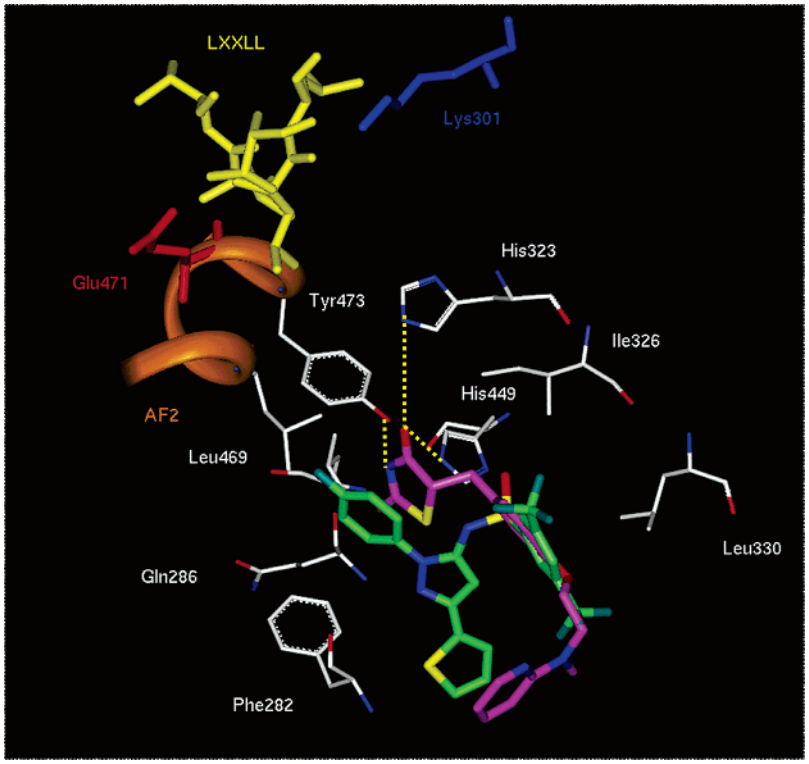

Figure 6. Superposition of the structures of compound **1** (green) and rosiglitazone (magenta) in the binding pocket of PPARγ. Rosiglitazone makes H-bonding interactions with His323, His449, Tyr473, and Ser289 whereas compound **1** has no H-bonding interactions with the protein. Moreover, the tail of rosiglitazone binds to an area near the entrance of the binding pocket whereas the interactions of compounds **1** with this entrance area are completely absent. However, compounds **1** form additional interactions with PPARγ in the hydrophobic pocket consisting of Phe282, Phe363, Leu453, Leu465, Leu469, and Gln286. AF-2 helix is shown as a ribbon drawing in orange. Lys301 and Glu471, the two residues forming the charge clamp, are colored as blue and red, respectively. The LXXLL motif of the coactivator is shown in yellow.

carboxylic group, makes strong H-bonding interactions with His323, His449, Tyr473, and, in some case, Ser289. This H-bonding interaction network with the protein is conserved in most of the PPARγ full agonists, and it is crucial to prompt the recruitment of coactivators upon the ligand binding as suggested by various reports.[18,19,22] As revealed in complex structures reported here, the two compounds lack thiazolidinedione or carboxylic moieties and thus have no H-bonding interactions with the protein. The absence of the conserved H-bonding pattern might explain why these ligands functioned as PPARγ partial agonists instead of full agonists. The linker of rosiglitazone and tesaglitazar occupies a narrow groove formed by Cys285, Ile326, Leu330, Leu333, Val339, and Met364 and makes hydrophobic interactions with the surrounding residues, particularly with Cys285. In compounds **1** and **2**, the sulfonamide and adjacent phenyl groups occupy a similar position to the linker in the full agonists. The interaction involves residues Leu330, Met364, and Cys285. Finally, the tail of rosiglitazone and tesaglitazar binds to an area near the entrance of the binding pocket whereas the interactions of compounds **1** and **2** with this entrance area were completely absent. However, compounds **1** and **2** form additional interactions with PPARγ deep in the hydrophobic pocket next to the AF-2 helix, consisting of Phe282, Phe363, Leu453, Leu465, Leu469, and Gln286. All aromatic rings of compounds **1** and **2**, except the phenyl ring connected to the sulfonamide in compound **2**, have extensive $\pi-\pi$ stacking and hydrophobic interactions with the surrounding protein residues, particularly with Phe363. Thus the interactions in this region play an important role in the binding and may compensate for loss of the interactions at the entrance.

Selectivity. The binding and transactivation assays show that both compound **1** and compound **2** are specific PPARγ agonists with no activity to PPARα or PPARδ. Structural alignment of these two complex structures with PPARα and PPARδ reveal that the side chains of Thr279 of PPARα and Thr288, the corresponding residue in PPARδ, would cause a steric clash with a CF_3 group in compound **1** or the fluorine atom of compound **2** (Figure 7A). Thr279 of PPARα and Thr288 of PPARδ are located at the entrance of the binding pocket, and the steric effect with compounds **1** and **2** might restrict their access to the binding pocket. In PPARγ, the corresponding residue Arg288 could shift away to allow the ligands access because of the highly flexible nature of the side chain. Second, a computer docking study shows that the interactions of compounds **1** and **2** with PPARγ are more favorable than with the other two PPAR subtypes. In the docking study it was assumed that Thr279 of PPARα and Thr288 of PPARδ could undergo conformational change to allow access of the ligands to the binding site in the similar position as PPARγ. However, the key residue Phe363 in PPARγ, that contributes $\pi-\pi$ stacking and important hydrophobic interactions with the aromatic rings of our compound, is replaced by Ile in PPARα and PPARδ (Figure 7B). The substitution of Phe by Ile would weaken the protein−ligand interaction and consequently decrease the binding affinity. Taking compound **2** as an example, the protein−ligand interaction energy calculated by DOCK is −15.00 (kcal/mol), −32.39 (kcal/mol) and −50.19 (kcal/mol) for PPARα, PPARδ, and PPARγ, respectively, suggesting the interactions of the compounds with PPARγ are more energetically favorable.

Studies in Vivo. The antidiabetic effect of compound **1** was further evaluated in vivo. In this study, KKA^y mice, which exhibit obesity, insulin resistance and relative type 2 diabetes-like symptoms,[25] were used. Compound **1** was administrated

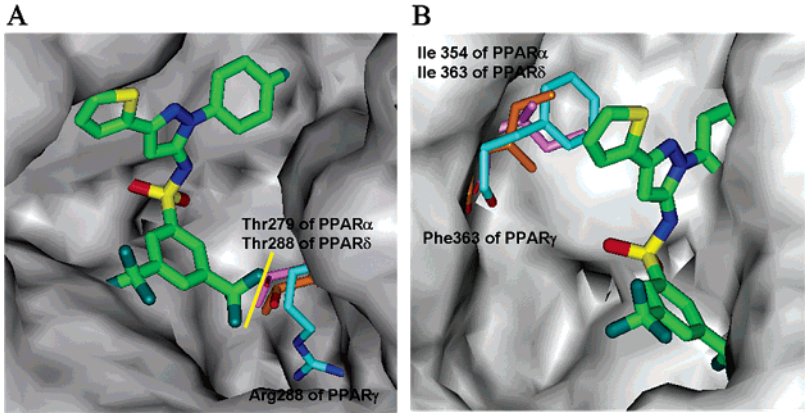

Figure 7. Proposed molecular determinants for compound **1**'s selectivity to PPARγ. (a) Overlay of PPARγ/compound **1** complex structure with PPARα and PPARδ. Thr279 of PPARα and Thr288 of PPARδ would cause a steric clash with a CF_3 group in compound **1**, shown as the yellow line. (b) The key residue Phe363 in PPARγ, that contributes $\pi-\pi$ stacking and important hydrophobic interactions with the aromatic rings of compound **1**, is replaced by Ile in PPARα and PPARδ.

Table 2. In Vivo Efficacy of Compound **1** in KKA$^{\gamma}$ Mice

	glucose level (mg/dl)		
	before treatment	after treatment	change (%)
vehicle control	298 ± 25[a]	271 ± 46[a]	
compound **1**	292 ± 24[b]	174 ± 14[b]	−35.7[c]

[a] Data are shown as the mean value ($n = 7$) ± SD. [b] Data are shown as the mean value ($n = 8$) ± SD. [c] $p = 0.05$ vs vehicle control.

daily at a dose of 30 mg/kg for 5 days. Plasma glucose levels was measured before the treatment (day 1), and 4 days after the treatment was initiated (day 4) (Table 2). Compound **1** decreased the blood glucose level by 35.7%, demonstrating its glucose-lowering efficacy in vivo.

Conclusion

In this study, structure-based virtual screening in which a combination of shape-based database search, docking study and analogue search is proven to be an efficient method to discover a novel class of PPARγ agonists. This technique enables the identification of compound **1**, a compound exhibiting high potency and specificity in vitro and showing efficacy in vivo. The structural biology studies revealed that compound **1** and its analogue, compound **2**, adopt a distinct binding mode and have no H-bonding interactions with PPARγ. The lack of H-bonding interaction with the protein provides the structural basis for their partial agonism since most full agonists form conserved H-bonding interactions with His323, His449 and Tyr473. This conserved H-bonding network stabilizes the AF-2 helix in a conformation to form a charge clamp between Arg301 and Glu471, which, consequently, positions the conserved LXXLL motif of coactivators to a hydrophobic site on the surface of PPARγ, resulting in the recruitment of coactivators.[18] In contrast, the absence of the H-bonding interactions of compound **1** and **2** with the receptor might affect the recruitment of coactivators thus decreasing their transcriptional activity. PPARγ partial agonists have gained more attention recently as they could reduce the side effects caused by full agonists.[16−17] The unique biological profiles of compound **1** make it as an attractive candidate for further development. The structure of PPARγ in complex with compound **1** and its analogue, compound **2**, could provide a rationale for the next generation of ligand design. Compound **1** is currently undergoing additional evaluation to further assess the potential for development for the treatment of type 2 diabetes.

Experimental Section

Shape-Based Database Searching. Shape-based database search was performed using the program Catalyst (version 4.7) developed in Accerlys Inc. (San Diego, CA). The bound conformation of compound **6** was retrieved from the PPARγ/**6** complex structure (PDB code: 1K74) and used as a query to screen Maybridge database, a commercially available compound database obtained from the Maybridge Chemical Company (Tintagel, Cornwall, UK). The pharmacophore shape tolerance parameters were set at the default setting in the Catalyst. The minimum and maximum percent extent for X, Y, and Z and the percent box volume match were set to 0.7 and 1.3, respectively. In addition, the minimum and maximum similarity tolerances were set to 0.5 and 1.

Molecular Docking of the Hit Compound to the Binding Pocket of PPARγ. The hit compound, **7** (*N*-[1-(4-fluorophenyl)-3-(2-thienyl)-1*H*-pyrazol-5-yl]-5-[5-(trifluoromethyl)isoxazol-3-yl]-thiophene-2-sulfonamide), was docked into the binding pocket of PPARγ by the program GOLD 2.0 (CCDC Software Limited, Cambridge, UK). The X-ray structure of PPARγ (PDB code 1K74),[19] excluding compound **6**, was chosen as a template protein for the docking study.

The binding pocket for the docking study was defined as a 15 Å radius sphere centered on Cys285. Twenty genetic algorithm (GA) runs were performed for compound **7** docking. For each GA run, 100 000 operations were operated on a population size of 100. The probability values for three types of operations; crossover, mutation, and migration, were set to 95%, 95%, and 10%, respectively. The annealing parameters of van der Waals and hydrogen bonding were set to 4.0, and 2.5, respectively, to allow a few bad bumps and poor hydrogen bonds at the beginning of a GA run. The "early-termination" option was applied to terminate docking if the root-mean-square deviation (rmsd) of the first three solutions was less than 1.5 Å. The template shape similarity constraint with the constraint weight set to 10 000 was used to improve the docking result using the **6** binding conformation as the template. The scoring function, GoldScore, implemented in GOLD was used to rank the docking positions of compound **7**.

Preparation of Recombinant PPARs and Ligand Binding Assay. The ligand binding domains of three PPARs (γ, α, and δ) were expressed in *E. coli* as glutathione S-transferase (GST) fusion proteins. The cDNAs of the ligand binding domain of PPARα (GenBank Accession number L02932), PPARδ (GenBank Accession number L07592), and PPARγ (GenBank Accession number U63415), respectively, were subcloned into pGEX-6P-1 bacterial expression vector (Amersham Biosciences, Piscataway, NJ). The ligand binding domains start from amino acid 167 for PPARα, 139 for PPARδ, and 203 for PPARγ, to the C-terminus of each protein. Recombinant fusion proteins were expressed and purified by GST-affinity chromatography following the procedures as suggested by the suppliers (Amersham Biosciences, Piscataway, NJ).

Scintillation proximity assays (SPA) were employed to measure the binding affinity of compounds to PPARγ and PPARδ.[26] SPA binding assays were performed in the buffer containing 10 mM Tris-Cl, pH 7.2, 1 mM EDTA, 10% (w/v) glycerol, 10 mM sodium molybdate, 1 mM dithiothreitol, 0.5 mM phenylmethylsulfonyl fluoride, 2 μg/mL benzamidine, and 0.1 mg/mL BSA. For the PPARγ-SPA, 60 Ci/mmol [^{3}H]rosiglitazone was dissolved in ethanol and diluted to a final concentration of 10 nM in the reaction mixtures. Recombinant GST-PPARγ was added to the SPA binding buffer to a final concentration of 5 nM. Protein A−yttrium silicate SPA beads were used following the dilution protocol according to supplier's recommendations (Amersham Biosciences, Piscataway, NJ). Goat anti-GST antibody diluted 1000-fold was in the assay reactions (Amersham Pharmacia Biotech). The GST-PPARγ, goat anti-GST antibody, test compounds, and SPA beads were mixed in a total volume of 80 μL per well in 96-well microtiter plates. After addition of 20 μL of [^{3}H]rosiglitazone to each well, the plates were incubated at 15 °C for 24 h under gentle shaking, and radioactivity was measured in a Packard Topcount scintillation counter. For the PPARδ-SPA, a similar procedure to that used for PPARγ-SPA was followed, but with [^{3}H]{3-chloro-4-[3-(7-propyl-3-trifluoromethylbenzo[*d*]isoxazol-6-yloxy)propylsulfanyl]phenyl}-acetic acid (L-783483), as the radiolabeled ligand. {3-Chloro-4-[3-(7-propyl-3-trifluoromethylbenzo[*d*]isoxazol-6-yloxy)propyl-sulfanyl]phenyl}acetic acid is known as a pan-PPAR ligand,[27] and the [^{3}H]{3-chloro-4-[3-(7-propyl-3-trifluoromethylbenzo[*d*]isoxazol-6-yloxy)propylsulfanyl]phenyl}acetic acid used in this study was synthesized in-house and radiolabeled by Perkin-Elmer Life Sciences (Boston, MA). For PPARα ligand binding, the charcoal binding assay was used.[27] In short, 2.5 nM [^{3}H]{3-chloro-4-[3-(7-propyl-3-trifluoromethylbenzo[*d*]isoxazol-6-yloxy)propylsulfanyl]-phenyl}acetic acid (79 Ci/mmol) and one of the test compounds were added to PPARα in binding buffer (10 mM Tris/ pH 7.2, 1mM EDTA, 10% glycerol, 7 μL/100 mL of β-mercaptoethanol, 10 mM sodium molybdate, 1 mM dithiothreitol, 2 μg/mL benzamide, and 0.5 mM phenylmethylsulfonyl fluoride). Solutions were incubated for 24 h at 4 °C in a final volume of 300 μL. Unbound ligand was then removed after a 10 min incubation with 200 μL of dextran/gelatin-coated charcoal on ice and by centrifugation at 3000 rpm for 10 min at 4 °C, and the supernatant was aliquoted out and counted in a Tri-Carg 2100 TR Liquid Scintillation Analyzer (Packard).

Cell Culture and PPAR Transactivation Assay. For plasmids used in transactivation assays, the ligand binding domains of three PPARs (γ, α, and δ) were individually fused with plasmid pSG424, a plasmid encoding the GAL4-DNA binding domain, to generate fusion constructs for PPAR-GAL4 chimeras. The fusion constructs were sequenced to confirm the accuracy of the chimeric genes. The reporter plasmid, pG5-TK-luc, was employed to respond to the GAL4-PPAR chimeric receptors. It contains five repeats of the GAL4 response element, upstream of a minimal thymidine kinase promoter and followed by the downstream luciferase gene (pG5-TK-luc). In addition, renilla luciferase gene encoded in pSV40-Ren under the control of the SV40 promoter was used as an internal control for transfection efficiency.

The transcriptional activation experiment was performed in Huh-7 cells. Huh-7 cells were maintained in Dulbecco's modified Eagle's medium (DMEM) containing 10% fetal bovine serum (Gemini Bio-Products, Woodland, CA), 100 units/mL penicillin G, and 100 mg/mL streptomycin sulfate. Cells were seeded at 1×10^5 cells/well in 24-well cell culture plates. After 24 h, transfection experiments were performed. The transfection mixture for each well contained 0.48 μL of FuGENE6 (Roche, Indianapolis, IN), 40 ng of pSG424-PPAR expression vector, 137 ng of pUAS(5 ×)-tk-luc reporter vector, and 0.245 ng of SV40-Ren as an internal control for transfection effeciency. Cells were incubated in the transfection mixture for 6 h followed by treatment with various concentrations of test compounds for 24 h. Cell lysates were then prepared using Reporter Lysis Buffer (Promega, Madison, WI) according to the manufacturer's instructions. Luciferase activity in cell extracts was measured using the Luciferase Assay kit (Promega, Madison, WI) in a SIRIUS-0 luminometer (Berthold Detection Systems, Pforzheim, Germany).

Adipocyte Differentiation Assay. 3T3-L1 pre-adipocytes were seeded at 3×10^5 cells/well in six-well cell culture plates. Cells were maintained in Dulbecco's modified Eagle's medium (DMEM) supplemented with 10% fetal calf serum (FCS, Gemini Bio-Products, Woodland, CA), 100 units/mL penicillin G, and 100 mg/mL streptomycin sulfate at 37 °C in a humidified atmosphere of 5% CO_2. When cells reached confluence, test compounds of various concentrations were added. After compound treatment for 4 to 5 days, the morphology of cells was visually examined under a light microscope. Meanwhile, to quantify the extent of adipocyte differentiation, cells were then stained with Oil-red O (Sigma, MO) as described previously. In short, cells were fixed in 10% formalin for at least 1 h and stained by immersion in Oil-red O for 2 h followed by rinsing with water. Cells were then incubated at 32 °C to remove excessive water.

Measurement of aP2 mRNA. The expression level of the aP2 gene in 3T3-L1 was used as a sensitive marker for adipogenesis. Confluent 3T3-L1 cells, in the absence or presence of test compounds, were incubated in culture medium with addition dexamethasone (1 μM) and insulin (150 nM) for 3 days. Total cellular RNA was extracted from cells using a Trizol RNA isolation kit (Invitrogen, Carlsbad, CA), and RNA concentration was estimated by absorbance at a wavelength of 260 nM. The mRNA of the aP2 gene (Genbank accession number: M13261) was quantified by a qPCR method with aP2 specific primers (forward primer 5′-CAA AAT GTG TGA TGC CTT TGT G-3′; reverse primer 5′-CTC TTC CTT TGG CTC ATG CC-3′) using the LightCycler (Roche Diagnostics GmbH, Mannheim, Germany). Statistical significance was evaluated using student's *t* test by comparing the aP2 emRNA levels from untreated cells with different treatment conditions. To compensate for multiple *t* tests, $P < 0.01$ was set as the level of significant difference.

Expression and Purification of PPARγ-LBD (PPARγ Ligand Binding Domain). PPARγ-LBD, starting from amino acid 207 to 477, was amplified by PCR and fused with glutathione S-transferase (GST) in the pGEX-6P-1 vector. Clones with the GST-PPARγ-LBD gene were transformed into BL21 (DE3) *E. coli* cells. The cells was grown at 37 °C for 2−3 h to reach $OD_{600} = 1$, followed by the addition of isopropyl β-D-thiogalactopytanoside (final concentration of 1.0 mM) to the culture and incubated for another 16 h at 27 °C. Cells were then harvested by centrifugation and resuspended in lysis buffer (50 mM Tris-Cl (pH 7.5), 1 mM EDTA and 0.1 mM PMSF, buffer A). After adding lysozyme to disrupt the cell membrane, the lysate was centrifuged at 19 000 rpm for 30 min at 4 °C. The supernatant was then filtered through a 0.45 μm filter and loaded onto Q-sepharose ion exchanger column (Hiprep 16/10 Q XL, Amersham Biosciences), preequilibrated with the buffer A. After washing, the bound protein was eluted with a linear gradient of 0% to 100% of buffer B (buffer A + 300 mM NaCl). The fractions containing GST-PPARγ-LBD were pooled, concentrated, and loaded into a GST affinity column (GSTPrep FF 16/10, Amersham Biosciences) equilibrated with PBS buffer. The column was first washed with PBS buffer to remove the unbound proteins and subsequently eluted by Tris buffer (50 mM tris (pH 7.5)) with 10 mM GSH to obtain the GST fusion protein. The eluate was then digested with PreScission protease (Amersham Biosciences) overnight at 4 °C. The GST tag was removed by a second passage through the GST affinity column (GSTPrep FF 16/10, Amersham Biosciences). The PPARγ-LBD was concentrated and exchanged into a buffer consisting of 20 mM Tris-Cl (pH 8.0), 5 mM DTT, 100 mM NaCl and 0.5 mM EDTA. The purity of PPARγ-LBD was checked by SDS−PAGE gels before crystallization.

Crystallization and Structure Determination. Crystals of the PPARγ/compound **1** and PPARγ/compound **2** were obtained by the hanging drop method. Typically, 25 μL PPARγ LBD (8.0 mg/mL in a buffer of 20 mM Tris-Cl (pH 8.0), 5 mM DTT, 100 mM NaCl and 0.5 mM EDTA) was mixed with 0.5 μL of compounds

(10 mM in a buffer of 20 mM Tris-Cl (pH 8.0), 5 mM DTT, 100 mM NaCl, and 0.5 mM EDTA) and equilibrated for 5 h on ice. The complex solution was then centrifuged for 1 min at 4 °C. The supernatant solution was withdrawn carefully by pipet and used for crystallization trials. In the crystallization trails, 1.5 μL of the complex solution was added to 1.5 μL of well solution. The well solution contained 25∼29% PEG3350 and 16 mM sodium citrate. The complex crystals were obtained after 3−7 days at 18 °C.

A crystal of about 0.2 mm in length was mounted in a 0.1−0.2 mm Cryoloop (Hampton Research, Inc.). The crystal was immersed briefly in a cryoprotectant containing 25% glycerol and then flash-frozen in liquid nitrogen. Diffraction data were collected at the SPring-8 on station SP12B2 and NSRRC on station BL17B2 with an ADSC Quantum4. The data were processed by DENZO[28] and reduced with SCALEPACK. The structure was solved by molecular replacement by MOLREP[29] using a monomer of published PPARγ LBD structure (PDB code: 2PRG) as the search model. The programs CNS[30] and REFMAC[31] were used for structural refinement and the addition of water molecules. Several rounds of refinement and model building were carried out with the program O.[32] The coordinates of the PPARγ/compound **1** (PDB code: 2G0H) and PPARγ/compound **2** (PDB code: 2G0G) have been deposited in the Protein Data Bank.

In Vivo Studies. Adult male KKAy mice were purchased from CLEA Japan Inc. and kept individually in plastic box cages containing paper bedding in environmentally controlled, clean-air rooms with a 12 h light cycle. Before the start of treatment, mice were grouped based on their nonfasting blood glucose levels. Each group contained seven or eight mice.

The mice were treated with compound **1** orally at a dose of 30 mg/kg once a day. Compound **1** was given as a dietary admixture at 0.01 or 0.001% in the diet. The mice were fed with the experimental diet and water ad libitum for 5 days. Mice of the vehicle control group were orally gavaged with 0.5% methyl cellulose (Sigma, St. Louis, MO). Blood samples were taken from the tail vein before treatment and 4 days after the treatment initiated and measured the glucose levels. The plasma glucose levels were determined enzymatically using ACCU-CHEK from Roche (Mannheim, Germany).

Acknowledgment. We thank Prof. Lindsay Sawyer (Institute of Cell & Molecular Biology, University of Edinburgh, UK) for fruitful discussions. We would also like to thank the staff at beamline SP12B2 at Spring-8 and 17B2 at NSRRC for technical assistance. This work was supported by National Health Research Institutes (Grant Nos. BP-093-PP-02, BP-093-PP-06, and BP-093-PP-02) and National Science Council of the Republic of China (Grant Nos. NSC 93-2323-B-007-001)

References

(1) Mangelsdorf, D. J.; Thummel, C.; Beato, M.; Herrlich, P.; Schutz, G.; Umesono, K.; Blumberg, B.; Kastner, P.; Mark, M.; Chambon, P.; Evans, R. M. The Nuclear Receptor Superfamily: The Second Decade. *Cell* **1995**, *83*, 835−839.

(2) Kliewer, S. A.; Sundseth, S. S.; Jones, S. A.; Brown, P. J.; Wisely, G. B.; Koble, C. S.; Devchand, P.; Wahli, W.; Willson, T. M.; Lenhard, J. M.; Lehmann, J. M. Fatty Acids and Eicosanoids Regulate Gene Expression Through Direct Interactions with Peroxisome Proliferator-Activated Receptors α and γ. *Proc. Natl. Acad. Sci. U.S.A.* **1997**, *94*, 4318−4323.

(3) Spiegelman, B. M. PPAR-γ: Adipogenic Regulator and Thiazolidinedione Receptor. *Diabetes* **1998**, *47*, 507−514.

(4) Willson, T. M.; Lambert, M. H.; Kliewer, S. A. Peroxisome Proliferator-Activated Receptor γ and Metabolic Disease. *Annu. Rev. Biochem.* **2001**, *70*, 341−367.

(5) Berger, J.; Moller, D. E. The Mechanisms of Action of PPARs. *Annu. Rev. Med.* **2002**, *53*, 409−435.

(6) Issemann, I.; Green, S. Activation of a Member of the Steroid Hormone Receptor Superfamily by Peroxisome Proliferators. *Nature* **1990**, *347*, 645−650.

(7) Oliver, W. R., Jr.; Shenk, J. L.; Snaith, M. R.; Russell, C. S.; Plunket, K. D.; Bodkin, N. L.; Lewis, M. C.; Winegar, D. A.; Sznaidman, M. L.; Lambert, M. H.; Xu, H. E.; Sternbach, D. D.; Kliewer, S. A.; Hansen, B. C.; Willson, T. M. A Selective Peroxisome Proliferator-Activated Receptor δ Agonist Promotes Reverse Cholesterol Transport. *Proc. Natl. Acad. Sci. U.S.A.* **2001**, *98*, 5306−5311.

(8) Park, B. H.; Vogelstein, B.; Kinzler, K. W. Genetic Disruption of PPARδ Decreases the Tumorigenicity of Human Colon Cancer Cells. *Proc. Natl. Acad. Sci. U.S.A.* **2001**, *98*, 2598−2603.

(9) Basu-Modak, S.; Braissant, O.; Escher, P.; Desvergne, B.; Honegger, P.; Wahli, W. Peroxisome Proliferator-Activated Receptor β Regulates Acyl-CoA Synthetase 2 in Reaggregated Rat Brain Cell Cultures. *J. Biol. Chem.* **1999**, *274*, 35881−35888.

(10) Wang, Y. X.; Zhang, C. L.; Yu, R. T.; Cho, H. K.; Nelson, M. C.; Bayuga-Ocampo, C. R.; Ham, J.; Kang, H.; Evans, R. M. Regulation of Muscle Fiber Type and Running Endurance by PPARδ. *PLoS Biol.* **2004**, *2*, E294.

(11) Lehmann, J. M.; Moore, L. B.; Smith-Oliver, T. A.; Wilkison, W. O.; Willson, T. M.; Kliewer, S. A. An Antidiabetic Thiazolidinedione is a High Affinity Ligand for Peroxisome Proliferator-Activated Receptor γ (PPAR γ). *J. Biol. Chem.* **1995**, *270*, 12953−12956.

(12) Devasthale, P. V.; Chen, S.; Jeon, Y.; Qu, F.; Shao, C.; Wang, W.; Zhang, H.; Cap, M.; Farrelly, D.; Golla, R.; Grover, G.; Harrity, T.; Ma, Z.; Moore, L.; Ren, J.; Seethala, R.; Cheng, L.; Sleph, P.; Sun, W.; Tieman, A.; Wetterau, J. R.; Doweyko, A.; Chandrasena, G.; Chang, S. Y.; Humphreys, W. G.; Sasseville, V. G.; Biller, S. A.; Ryono, D. E.; Selan, F.; Hariharan, N.; Cheng, P. T. Design and Synthesis of *N*-[(4-Methoxyphenoxy)carbonyl]-*N*-[[4-[2-(5-methyl-2-phenyl-4-oxazolyl)ethoxy]phenyl]methyl]glycine [Muraglitazar/BMS-298585], a Novel Peroxisome Proliferator-Activated Receptor α/γ Dual Agonist with Efficacious Glucose and Lipid-Lowering Activities. *J. Med. Chem.* **2005**, *48*, 2248−2250.

(13) Hegarty, B. D.; Furler, S. M.; Oakes, N. D.; Kraegen, E. W.; Cooney, G. J. Peroxisome Proliferator-Activated Receptor (PPAR) Activation Induces Tissue-Specific Effects on Fatty Acid Uptake and Metabolism In Vivo-A Study Using the Novel PPARα/γ Agonist Tesaglitazar. *Endocrinology* **2004**, *145*, 3158−3164.

(14) Lohray, B. B.; Lohray, V. B.; Bajji, A. C.; Kalchar, S.; Poondra, R. R.; Padakanti, S.; Chakrabarti, R.; Vikramadithyan, R. K.; Misra, P.; Juluri, S.; Mamidi, N. V.; Rajagopalan, R. (−)3-[4-[2-(Phenoxazin-10-yl)ethoxy]phenyl]-2-ethoxypropanoic acid [(−)DRF 2725]: A Dual PPAR Agonist with Potent Antihyperglycemic and Lipid Modulating Activity. *J. Med. Chem.* **2001**, *44*, 2675−2678.

(15) Doebber, T. W.; Kelly, L. J.; Zhou, G.; Meurer, R.; Biswas, C.; Li, Y.; Wu, M. S.; Ippolito, M. C.; Chao, Y. S.; Wang, P. R.; Wright, S. D.; Moller, D. E.; Berger, J. P. MK-0767, A Novel Dual PPARα/γ Agonist, Displays Robust Antihyperglycemic and Hypolipidemic Activities. *Biochem. Biophys. Res. Commun.* **2004**, *318*, 323−328.

(16) Berger, J. P.; Petro, A. E.; Macnaul, K. L.; Kelly, L. J.; Zhang, B. B.; Richards, K.; Elbrecht, A.; Johnson, B. A.; Zhou, G.; Doebber, T. W.; Biswas, C.; Parikh, M.; Sharma, N.; Tanen, M. R.; Thompson, G. M.; Ventre, J.; Adams, A. D.; Mosley, R.; Surwit, R. S.; Moller, D. E. Distinct Properties and Advantages of a Novel Peroxisome Proliferator-Activated Protein γ Selective modulator. *Mol. Endocrinol.* **2003**, *17*, 662−676.

(17) Reifel Miller, A.; Otto, K.; Hawkins, E.; Barr, R.; Bensch, W. R.; Bull, C.; Dana, S.; Klausing, K.; Martin, J.-A.; Rafaeloff-Phail, R.; Rafizadeh-Montrose, C.; Rhodes, G.; Robey, R.; Rojo, I.; Rungta, D.; Snyder, D.; Wilbur, K.; Zhang, T.; Zink, R.; Warshawsky, A.; Brozinick, J. T. A PPARα/γ Dual Agonist with a Unique In Vitro Profile and Potent Glucose and Lipid Effects in Rodent Models of Type 2 Diabetes and Dyslipidemia. *Mol. Endocrinol.* **2005**, *19*, 1593−1605.

(18) Nolte, R. T.; Wisely, G. B.; Westin, S.; Cobb, J. E.; Lambert, M. H.; Kurokawa, R.; Rosenfeld, M. G.; Willson, T. M.; Glass, C. K.; Milburn, M. V. Ligand Binding and Co−Activator Assembly of the Peroxisome Proliferator-Activated Receptor-γ. *Nature* **1998**, *395*, 137−143.

(19) Xu, H. E.; Lambert, M. H.; Montana, V. G.; Plunket, K. D.; Moore, L. B.; Collins, J. L.; Oplinger, J. A.; Kliewer, S. A.; Gampe, R. T., Jr.; McKee, D. D.; Moore, J. T.; Willson, T. M. Structural Determinants of Ligand Binding Selectivity Between the Peroxisome Proliferator-Activated Receptors. *Proc. Natl. Acad.* Sci. *U.S.A.* **2001**, *98*, 13919−13924.

(20) Mahindroo, N.; Huang, C. F.; Peng, Y. H.; Wang, C. C.; Liao, C. C.; Lien, T. W.; Chittimalla, S. K.; Huang, W. J.; Chai, C. H.; Prakash, E.; Chen, C. P.; Hsu, T. A.; Peng, C. H.; Lu, I. L.; Lee, L. H.; Chang, Y. W.; Chen, W. C.; Chou, Y. C.; Chen, C. T.; Goparaju, C. M. V.; Chen, Y. S.; Lan, S. J.; Yu, M. C.; Chen, X.; Chao, Y. S.; Wu, S. Y.; Hsieh, H. P. Novel Indole-Based Peroxisome Proliferator-Activated Receptor Agonists: Design, SAR, Structural Biology, and Biological Activities. *J. Med. Chem.* **2005**, *48*, 8194−8208.

(21) Mahindroo, N.; Wang, C. C.; Liao, C. C.; Huang, C. F.; Lu, I. L.; Lien, T. W.; Peng, Y. H.; Huang, W. J.; Lin, Y. T.; Hsu, M. C.; Lin, C. H.; Tsai, C. H.; Hsu, J. T. A.; Chen, X.; Lyu, P. C.; Chao, Y. S.; Wu, S. Y.; Hsieh, H. P. Indol-1-yl Acetic Acids as Peroxisome Proliferator-Activated Receptor Agonists: Design, Synthesis, Structural Biology, and Molecular Docking Studies. *J. Med. Chem.* **2006**, *49*, 1212−1216.

(22) Cronet, P.; Petersen, J. F. W.; Folmer, R.; Blomberg, N.; Sjoblom, K.; Karlsson, U.; Lindstedt, E.-L.; Bamberg, K. Structure of the PPARα and -γ Ligand Binding Domain in Complex with AZ 242; Ligand Selectivity and Agonist Activation in the PPAR Family. *Structure* **2001**, *9*, 699−706.

(23) Oberfield, J. L.; Collins, J. L.; Holmes, C. P.; Goreham, D. M.; Cooper, J. P.; Cobb, J. E.; Lenhard, J. M.; Hull-Ryde, E. A.; Mohr, C. P.; Blanchard, S. G.; Parks, D. J.; Moore, L. B.; Lehmann, J. M.; Plunket, K.; Miller, A. B.; Milburn, M. V.; Kliewer, S. A.; Willson, T. M. A Peroxisome Proliferator-Activated Receptor γ Ligand Inhibits Adipocyte Differentiation. *Proc. Natl. Acad. Sci. U.S.A.* **1999**, *96*, 6102−6106.

(24) Gampe, J.; Robert T.; Montana, V. G.; Lambert, M. H.; Miller, A. B.; Bledsoe, R. K.; Milburn, M. V.; Kliewer, S. A.; Willson, T. M.; Xu, H. E. Asymmetry in the PPARγ/RXRα Crystal Structure Reveals the Molecular Basis of Heterodimerization among Nuclear Receptors. *Mol. Cell* **2000**, *5*, 545−555.

(25) Iwatsuka, H.; Shino, A.; Suzuoki, Z. General Survey of Diabetic Features of Yellow KK Mice. *Endocrinol. Jpn.* **1970**, *17*, 23−35.

(26) Elbrecht, A.; Chen, Y.; Adams, A.; Berger, J.; Griffin, P.; Klatt, T.; Zhang, B.; Menke, J.; Zhou, G.; Smith, R. G.; Moller, D. E. L-764406 is a Partial Agonist of Human Peroxisome Proliferator-Activated Receptor γ. The Role of Cys313 in Ligand Binding. *J. Biol. Chem.* **1999**, *274*, 7913−7922.

(27) Berger, J.; Leibowitz, M. D.; Doebber, T. W.; Elbrecht, A.; Zhang, B.; Zhou, G.; Biswas, C.; Cullinan, C. A.; Hayes, N. S.; Li, Y.; Tanen, M.; Ventre, J.; Wu, M. S.; Berger, G. D.; Mosley, R.; Marquis, R.; Santini, C.; Sahoo, S. P.; Tolman, R. L.; Smith, R. G.; Moller, D. E. Novel Peroxisome Proliferator-Activated Receptor (PPAR) γ and PPARδ Ligands Produce Distinct Biological Effects. *J. Biol. Chem.* **1999**, *274*, 6718−6725.

(28) Otwinowski, Z.; Minor, W. Processing of X-ray Diffraction Data Collected in Oscillation Mode. *Methods Enzymol.* **1997**, *276*, 307−326.

(29) Vagin A, T. A. MOLREP: An Automated Program for Molecular Replacement. *J. Appl. Crystallogr.* **1997**, *30*, 1022−1025.

(30) Brunger, A. T.; Adams, P. D.; Clore, G. M.; Delano, W. L.; Gros, P.; Grosse-Kunstleve, R. W.; Jiang, J.-S.; Kuszewski, J.; Nilges, M.; Pannu, N. S.; Read, R. J.; Rice, L. M.; Simonson, G. L.; Warren, T.; Badger, J.; Berard, D.; Kumar, R. A.; Szalma, S.; Yip, P.; Griesinger, C.; Junker, J. Crystallography and NMR System: A New Software Suite for Macromolecular Structure Determination. *Acta Crystallogr.* **1998**, *D54*, 905−921.

(31) Murshudov, G. N.; Vagin, A. A.; Dodson, E. J. Refinement of Macromolecular Structures by the Maximum-Likelihood Method. *Acta Crystallogr.* **1997**, *D53*, 240−255.

(32) Jones, T. A.; Zou, J. Y.; Cowan, S. W.; Kjeldgaard, M. Improved Methods for Building Protein Models in Electron Density Maps and the Location of Errors in these Models. *Acta Crystallogr.* **1991**, *A47*, 110−119.

JM051129S